




Communication

Phytochemical Investigation of Bioactive Compounds from White Kidney Beans (Fruits of *Phaseolus multiflorus* var. *Albus*): Identification of Denatonium with Osteogenesis-Inducing Effect

Yong Hoon Lee ^{1,†}, Joo-Hyun Hong ^{1,†}, Kun Hee Park ², Seon-Hee Kim ³, Jin-Chul Kim ⁴ , Do Hoon Kim ⁵, Yu Hwa Park ⁵, Kye Wan Lee ⁵, Jung Kyu Kim ^{6,*}  and Ki Hyun Kim ^{1,*} 

¹ School of Pharmacy, Sungkyunkwan University, Suwon 16419, Korea; yhl2090@naver.com (Y.H.L.); ehong@skku.edu (J.-H.H.)

² Department of Food Science and Biotechnology, Sungkyunkwan University, Suwon 16419, Korea; soske@skku.edu

³ Sungkyun Biotech Co., Ltd., Suwon 16419, Korea; seonhee31@gmail.com

⁴ Natural Product Informatics Research Center, KIST Gangneung Institute of Natural Products, Gangneung 25451, Korea; jckim@kist.re.kr

⁵ R&D Center, Dongkook Pharm. Co., Ltd., Suwon 16229, Korea; kdh2@dkpharm.co.kr (D.H.K.); pyh@dkpharm.co.kr (Y.H.P.); lkw1@dkpharm.co.kr (K.W.L.)

⁶ School of Chemical Engineering, Sungkyunkwan University, Suwon 16419, Korea

* Correspondence: legkim@skku.edu (J.K.K.); khkim83@skku.edu (K.H.K.); Tel.: +82-31-290-7254 (J.K.K.); +82-31-290-7700 (K.H.K.)

† These authors contributed equally to this study.



Citation: Lee, Y.H.; Hong, J.-H.; Park, K.H.; Kim, S.-H.; Kim, J.-C.; Kim, D.H.; Park, Y.H.; Lee, K.W.; Kim, J.K.; Kim, K.H. Phytochemical Investigation of Bioactive Compounds from White Kidney Beans (Fruits of *Phaseolus multiflorus* var. *Albus*): Identification of Denatonium with Osteogenesis-Inducing Effect. *Plants* **2021**, *10*, 2205. <https://doi.org/10.3390/plants10102205>

Academic Editor: Daniela Rigano

Received: 27 September 2021

Accepted: 14 October 2021

Published: 17 October 2021

Publisher's Note: MDPI stays neutral with regard to jurisdictional claims in published maps and institutional affiliations.



Copyright: © 2021 by the authors. Licensee MDPI, Basel, Switzerland. This article is an open access article distributed under the terms and conditions of the Creative Commons Attribution (CC BY) license (<https://creativecommons.org/licenses/by/4.0/>).

Abstract: *Phaseolus multiflorus* var. *albus* (Leguminosae), commonly known as “white kidney bean”, is a twining perennial vine whose fruit has been used as a popular food worldwide owing to its high nutritional content, in terms of proteins, carbohydrates, fats, and vitamins. As part of our ongoing study to investigate novel bioactive components from various natural resources, a phytochemical investigation of the extract of *P. multiflorus* var. *albus* fruits resulted in the isolation of three phenolic compounds (1–3) and one dipeptide (4). The chemical structures of the compounds (1–4) were determined through 1D and 2D nuclear magnetic resonance spectroscopy and high-resolution-liquid chromatography–mass spectrometry; they were identified as denatonium (1), *trans*-ferulic acid ethyl ester (2), eugenin (3), and α -L-glutamyl-L-Leucine (4). Intriguingly, denatonium (1) is known to be the most bitter chemical compound. To the best of our knowledge, denatonium (1) was identified from natural sources for the first time, and compounds 2–4 were reported for the first time from *P. multiflorus* var. *albus* in this study; however, compound 2 turned out to be an artifact produced by an extraction with ethanol. The isolated compounds 1–4 were tested for their regulatory effects on the differentiation between osteogenesis and adipogenesis of mesenchymal stem cells (MSCs). Compound 4 slightly suppressed the adipogenic differentiation of MSCs, and compounds 1 and 4 stimulated osteogenic differentiation, unlike the negative control. These findings provide experimental evidence that compounds 1 and 4 may induce the osteogenesis of MSCs and activate bone formation.

Keywords: *Phaseolus multiflorus* var. *albus*; Leguminosae; white kidney bean; denatonium; osteogenesis

1. Introduction

Phaseolus multiflorus var. *albus*, also known as white kidney bean, is a twining perennial vine belonging to the family Leguminosae. It has been cultivated for many purposes worldwide, especially in China [1]. Historically, leguminous plants have been popular worldwide because they are abundant in proteins (16–33%), minerals, carbohydrates, fats, vitamins, and phytoestrogens [1,2]. Pharmacological studies of plants belonging

to the genus *Phaseolus* have reported that its extracts exhibit various therapeutic properties, including antidiabetic [1,2], antiobesogenic [3], antiproliferative [4], antioxidant, and gastroprotective activities [5]. In addition, previous studies on plants belonging to the genus *Phaseolus* have shown that their nutritional contents possess insecticidal, immunomodulatory, antitumor, and antifungal activities [4,5]. Previous biological studies on *P. multiflorus* var. *albus* reported that white kidney bean (*P. multiflorus* var. *albus*) treatments induced glucose reduction and weight loss in a diabetes-induced mouse model compared to the control group [6]. In this context, many clinical trials on the antiobesity effect of *P. multiflorus* var. *albus* have revealed that the ingestion of white kidney beans induces weight loss and waist circumference reduction [7]. In a recent study, *P. multiflorus* var. *albus* extract showed dose-dependent inhibitory activity against α -amylase [8]. Despite the health benefits of *P. multiflorus* var. *albus* extract, few studies have been carried out on its chemical constituents. Only a few previous phytochemical investigations of *P. multiflorus* have shown the presence of gibberellins A₁, A₅, A₆, A₈, and phaseic acid as plant hormones with growth-promoting activity [9–12].

Therefore, as part of our ongoing study to investigate novel bioactive components from various natural resources [13–19], we investigated the potential bioactive components from the extract of *P. multiflorus* var. *albus* fruits. In the current study, the phytochemical constituents of the ethanolic extract of *P. multiflorus* var. *albus* fruits were isolated, resulting in the isolation of three phenolic compounds (1–3) and one dipeptide (4). The chemical structures of compounds (1–4) were clearly elucidated through 1D and 2D nuclear magnetic resonance (NMR) spectroscopic data and high-resolution electrospray ionization (HR-ESI) liquid chromatography–mass spectrometry (LC/MS) analyses. In addition, the isolated compounds, 1–4, were tested for their regulatory effects on the differentiation between osteogenesis and adipogenesis of mesenchymal stem cells (MSCs). Herein, we report the isolation and structural determination of the isolated compounds 1–4 as well as their regulatory effects on the differentiation of MSCs.

2. Results and Discussion

2.1. Isolation of Compounds

The fruits of *P. multiflorus* var. *albus* were extracted with 30% ethanol/H₂O. The resultant extract was suspended for solvent partitioning in water and then fractionated with four solvents, which afforded hexane-soluble (31.4 mg), dichloromethane-soluble (195.7 mg), ethyl acetate-soluble (49.3 mg), and *n*-butanol-soluble (2.4 g) fractions. The LC/MS-based analysis combined with our in-house built UV library and thin-layer chromatography (TLC) analysis of the solvent-partitioned fractions suggested that the BuOH-soluble fraction contained the majority of the organic acid derivatives. A phytochemical investigation of the solvent-partitioned fractions was conducted under monitoring by TLC and LC/MS-based analysis using repeated column chromatography with silica gel 60, RP-C₁₈ silica gel, and Sephadex LH-20, and high-performance liquid chromatography (HPLC) (Figure 1). The final semi-preparative HPLC separation afforded a phenolic compound (1) from the EA-soluble fraction, two phenolic compounds (2 and 3) from the hexane-soluble fraction, and one dipeptide (4) from the *n*-butanol-soluble fraction (Figure 2).

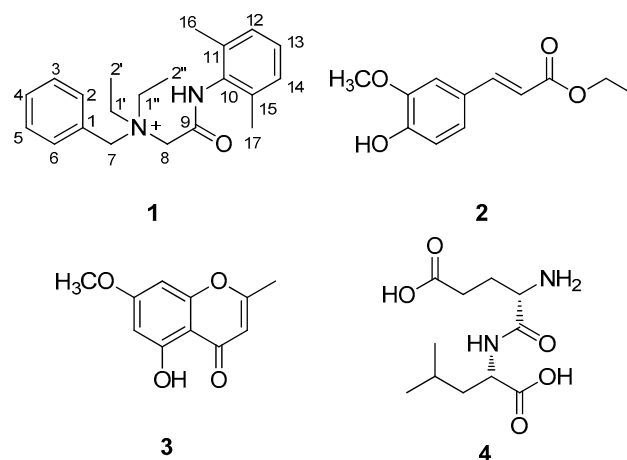
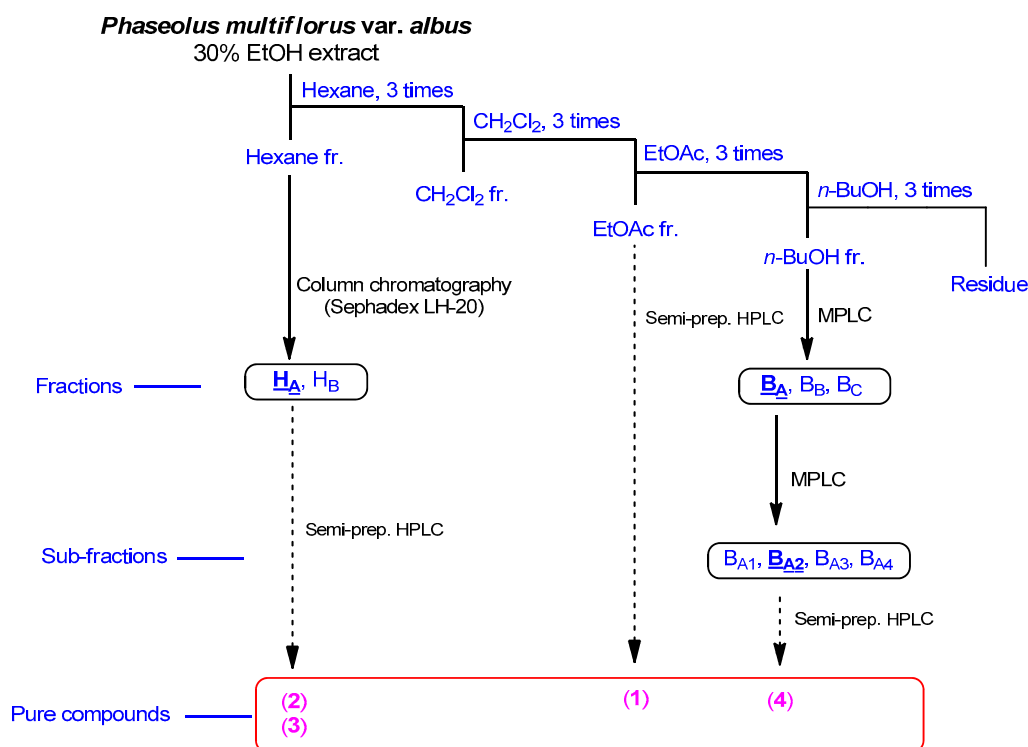


Figure 2. Chemical structures of compounds 1–4.

2.2. Elucidation of Compound Structures

Compound **1** was isolated as a white amorphous powder. The molecular formula was deduced to be $C_{21}H_{29}N_2O^+$ from the molecular ion peak $[M]^+$ at m/z 325.2282 (calculated for $C_{21}H_{29}N_2O^+$, 325.2274) in the positive-ion mode of HRESIMS (Figure S1). The 1H NMR spectrum of **1** (Table 1, Figure S2) displayed the presence of the characteristic signals of two aromatic proton sets of a monosubstituted aromatic ring at δ_H 7.64 (2H, t, $J = 7.5$ Hz), δ_H 7.62 (1H, t, $J = 7.5$ Hz), and δ_H 7.58 (2H, t, $J = 7.5$ Hz); 1,2,6-trisubstituted aromatic ring at δ_H 7.18 (1H, t, $J = 7.0$ Hz) and δ_H 7.17 (2H, d, $J = 7.0$ Hz); two pairs of relatively deshielded methylene groups at δ_H 4.94 (2H, s) and δ_H 4.16 (2H, s); two symmetric methyl groups at δ_H 2.30 (6H, s); and another two pairs of ethyl groups at δ_H 3.67 (4H, m) and δ_H 1.56 (6H, t, $J = 7.5$ Hz). The ^{13}C NMR data of **1** (Table 1, Figure S3), assigned with the aid of the HSQC (Figure S5) and HMBC experiments (Figure S6) confirmed 21 carbon signals composed of four methyl groups at δ_C 8.4 ($2 \times C$) and δ_C 18.7 ($2 \times C$); four methylene

carbons at δ_C 54.9 ($2 \times C$), δ_C 55.7, and δ_C 63.4; 12 aromatic carbons (δ_C 128.7, 129.1, 129.5 ($2 \times C$), 130.7 ($2 \times C$), 132.3, 134.1 ($2 \times C$), 134.2, 136.7 ($2 \times C$)); and a carbonyl carbon at δ_C 164.1. The partial structures of **1** were determined by 2D NMR experiments (1H - 1H COSY and HMBC). The gross structure of **1** was finally elucidated by the characteristic NMR signals, and its molecular formula ($C_{21}H_{29}N_2O^+$) was confirmed by HRESIMS. The 1H - 1H COSY correlations (Figure S4) between H-2/H-3/H-4/H-5/H-6 as well as the HMBC correlations of H-2(H-6)/C-7 (δ_C 63.4) and H₂-7/C-1, C-2, and C-3 verified the presence of benzyl functionality (Figure 3). Furthermore, the methylene of H₂-7 showed HMBC correlations with three other carbons: C-8 (δ_C 55.7), C-1' (δ_C 54.9), and C-1'' (δ_C 54.9) (Figure 3), providing evidence that a quaternary atom linking C-7, C-8, C-1', and C-1'' is present. Based on the 1H - 1H COSY spectrum of H₂-1'/H₂-2' and H₂-1''/H₂-2'' and the HMBC correlations of H₂-1'/H₂-1'' with C-2'/C-2'', along with their symmetric NMR signals, the two ethyl units were assigned and confirmed to be attached to the quaternary atom by the HMBC correlations of H₂-1'/H₂-1'' with C-7 and C-8. The relatively deshielded methylene carbon NMR signals of C-7, C-8, C-1', and C-1'' and the markedly diminished intensity of the carbon NMR signals observed for C-1', and C-1'' at δ_C 54.9 confirmed that the quaternary atom linking them could be a quaternary ammonium cation, which finally led to the partial structure of A (Figure 3). Another spin system was observed as a cross-peak between H-12/H-13/H-14 in the 1H - 1H COSY spectrum, representing the 1,2,6-trisubstituted aromatic ring, which was assigned to the 2,6-dimethylated benzene as the partial structure of B by the HMBC correlations of H-12(H-14)/C-10, H-13/C-11(C-15), C-16(C-17)/C-10, C-11, and C-12 (Figure 3). Finally, the connectivity through the amide bond between the two partial structures of A and B was suggested by the C=O and NH moieties remaining from the molecular formula ($C_{21}H_{29}N_2O^+$) of **1**, the detected HMBC correlation of H₂-8/C-9 (δ_C 164.1), and the characteristic ^{13}C chemical shifts of C-8 (δ_C 55.7) and C-10 (δ_C 134.2), although the key HMBC correlation between C-9 and C-10 was missing in **1** due to the absence of protons. Accordingly, the complete structure of **1** was established, as shown in Figure 1, and it was identified to be denatonium.

Table 1. 1H and ^{13}C NMR data of compound **1** in CD₃OD (δ in ppm, 850 MHz and 212.5 MHz for 1H and ^{13}C , respectively) ^a.

Position	Denatonium (1)	
	δ_H (J in Hz)	δ_C
1		128.7 C
2	7.64, d (7.5)	134.1 CH
3	7.58, t (7.5)	130.7 CH
4	7.62, t (7.5)	132.3 CH
5	7.58, t (7.5)	130.7 CH
6	7.64, d (7.5)	134.1 CH
7	4.94, s	63.4 CH ₂
8	4.16, s	55.7 CH ₂
9		164.1 C
10		134.2 C
11		136.7 C
12	7.17, d (7.0)	129.5 CH
13	7.18, t (7.0)	129.1 CH
14	7.17, d (7.0)	129.5 CH
15		136.7 C
16	2.30, s	18.7 CH ₃
17	2.30, s	18.7 CH ₃
1'	3.67, m	54.9 CH ₂
2'	1.56, t (7.5)	8.4 CH ₃
1''	3.67, m	54.9 CH ₂
2''	1.56, t (7.5)	8.4 CH ₃

^a Coupling constants (Hz) are given in parentheses. ^{13}C NMR assignments were based on HSQC, 1H - 1H COSY, and HMBC experiments.

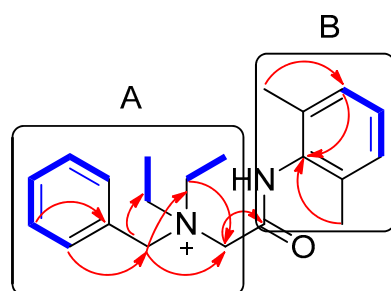


Figure 3. Key ^1H - ^1H COSY (—) and HMBC (↷) correlations of compound **1**. A and B represent two partial structures.

The structures of the known compounds (Figure 1) were determined to be *trans*-ferulic acid ethyl ester (**2**) [20], eugenin (**3**) [21], and α -L-glutamyl-L-Leucine (**4**) [22] by comparing their NMR spectroscopic data with those previously reported in the literature and MS data obtained from the LC/MS analysis. To the best of our knowledge, denatonium (**1**) was identified from a natural source for the first time, and compounds **2–4** were reported for the first time from *P. multiflorus* var. *albus* in this study. In natural product chemistry, it is important to take the necessary precautions during the isolation work in order to minimize the possibility of unexpected artifact isolation [23]. To verify whether compounds **1–4** were genuine natural compounds or artifacts, *P. multiflorus* var. *albus* was extracted with 80% methanol (*v/v*) for 10 h, and the resultant methanolic extract was subjected to LC/MS analysis. As a result, there was no peak with a molecular ion corresponding to compound **2** in the methanolic extract, whereas compounds **1**, **3**, and **4** were detected, suggesting that compound **2** was an artifact produced by the extraction with ethanol. In addition, to confirm that the isolated denatonium (**1**) is a natural compound, the methanol used for extraction was analyzed using ultra-performance liquid chromatography (UPLC) quadrupole time-of-flight (Q-TOF) high-resolution (HR)-MS because methanol can possess denatonium as a component. As a result, there was no detected peak for denatonium in the methanol solvent that we used for extraction (Figure S7), suggesting that the methanol used does not contain denatonium and the isolated denatonium can be a genuine natural compound.

Intriguingly, denatonium (benzyl-[2-(2,6-dimethylanilino)-2-oxoethyl]-diethylazanium), which is odorless and chemically stable, was found during research on local anesthetics in 1958 [24]. Since then, it has been widely used in various industries, such as cosmetics, pharmaceuticals, and material industries [25]. Interestingly, its bitterness and aversive taste have served to prevent young children from swallowing small household items, including toys and game packs, which has allowed denatonium to be widely employed in many household items. Denatonium is known to be one of the most bitter chemical compounds; thus, it was nominated in the Guinness Book of World Records as one of the most bitter compounds that people can use [26].

2.3. Evaluation of the Biological Activities of Compounds **1–4**

MSCs are pluripotent cells in bone marrow that are known to differentiate into osteocytes and adipocytes. As microenvironmental changes cause alterations in the regulation of gene expression in MSC differentiation, the alterations of related gene expression might disturb the balance between adipocyte progenitor and osteoprogenitor cells in patients with osteoporosis [27–29]. Thus, a therapy that can regulate gene expression in MSCs would be promising for the management of postmenopausal osteoporosis. To determine the regulatory effects of compounds **1–4** on MSC differentiation between adipogenesis and osteogenesis, all the compounds were examined for their effects on the differentiation of murine MSCs into adipocytes or osteoblasts. The murine MSC line C3H10T1/2 was treated with 20 μM of the compounds during adipogenesis, and the differentiated cells were stained with Oil Red O (ORO). Compound **4** slightly reduced the formation of lipid droplets, resulting in fewer ORO-stained cells, compared to the normally differentiated adipocytes (Figure 4A,B). In addition, C3H10T1/2 cells were cultured in osteogenesis-

inducing media in the presence of compounds 1–4. The cells were then stained for alkaline phosphatase (ALP), which is considered a distinctive marker of osteoblast differentiation [30]. Cells treated with compounds 1 and 4 showed slightly higher staining intensity and ALP enzyme activity than the negative control group (Figure 4C,D).

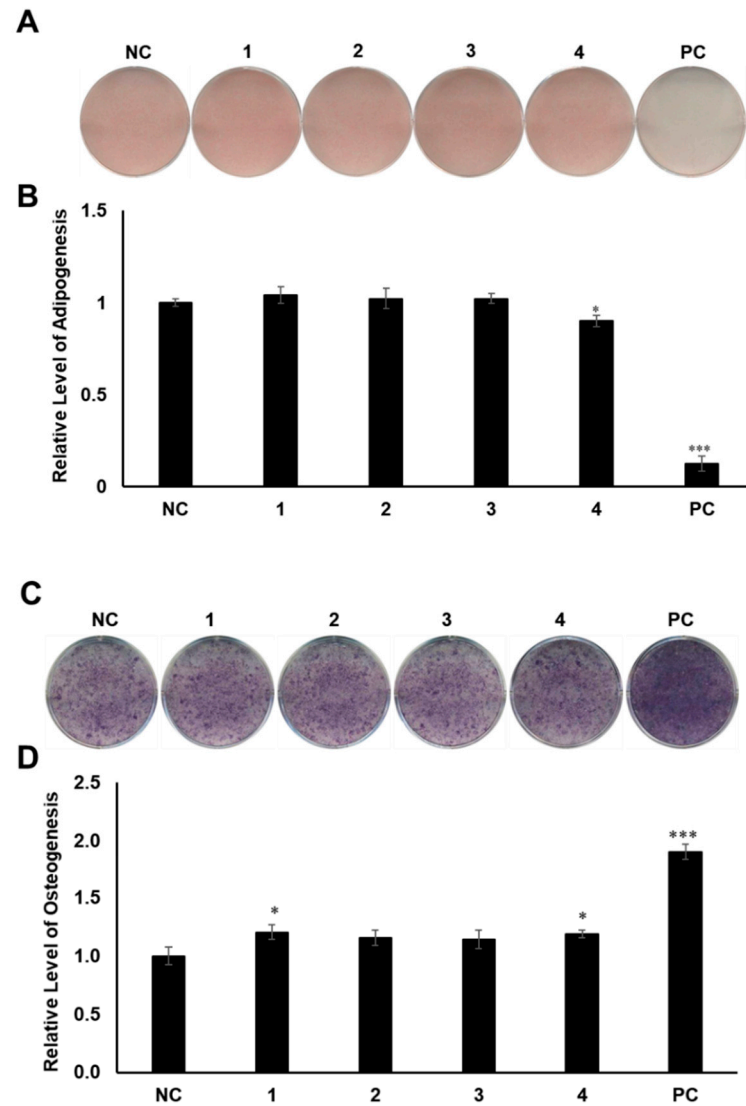


Figure 4. The effects of compounds 1–4 on the differentiation of mesenchymal stem cells (MSCs) toward adipocytes and osteoblasts. (A) Suppressive effects of compounds 1–4 on the adipogenic differentiation of MSCs. C3H10T1/2 cells were treated with 20 μ M of compounds 1–4. After adipogenic differentiation, the cells were stained with Oil Red O (ORO). (B) The intensity of stained lipid droplets was quantitatively examined. (C) Stimulatory effects of compounds 1–4 on osteogenic differentiation of MSCs. Fully differentiated C3H10T1/2 cells were stained with alkaline phosphatase (ALP) on day 9 post osteogenic differentiation with 20 μ M compounds 1–4. (D) ALP enzyme activity was determined in osteogenically differentiated C3H10T1/2 cells treated with compounds 1–4. The values were calculated relatively by setting the untreated negative control (NC) to 1. Resveratrol (20 μ M) and oryzativol A (5 μ M) were added to the experimental set for adipogenesis and osteogenesis, respectively, as a positive control (PC). * denotes $p < 0.05$ and *** denotes $p < 0.001$.

Compounds 1 and 4 showed the regulatory effects on the differentiation between osteogenesis and adipogenesis of MSCs (Figure 4). Among the active compounds, compound 4 was not sufficient for further experiments to examine its effects. To test the effects of compound 1 on osteogenic differentiation, C3H10T1/2 cells were stained with ALP

(Figure 5A), and ALP enzyme activity was measured (Figure 5B). Our results indicated that increased concentrations of compound 1 led to the formation of darker-colored cells (Figure 5A), which indicated that the treated cells exhibited greater promotion of bone differentiation than the control group (Figure 5B). Moreover, compound 1 slightly enhanced the gene expression of *ALP* (Figure 5C) and osteopontin (*OPN*) (Figure 5D), which are osteogenesis-related factors, during osteogenic differentiation in a dose-dependent manner.

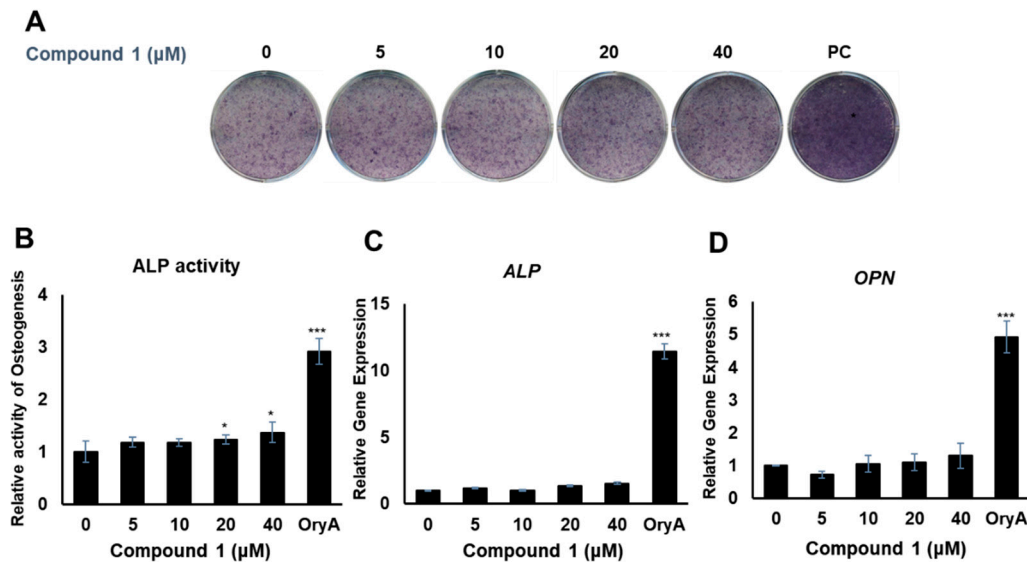


Figure 5. The effects of compound 1 on osteogenic differentiation. C3H10T1/2 cells were treated with sequential concentrations (5, 10, 20, and 40 μM) of compound 1 during osteogenic differentiation. The effects of compound 1 were evaluated through ALP staining (A). The cells were evaluated by measuring the ALP activity (B). The mRNA expression of *ALP* (C) and *OPN* (D) was measured by real-time PCR. Oryzativol A (OryA) at a concentration of 5 μM was used as a positive control (PC). * denotes $0.01 < p < 0.05$ and *** denotes $p < 0.001$.

3. Materials and Methods

3.1. Plant Material

Plant material (fruits of *P. multiflorus* var. *albus*) was provided by Dongkook Pharm. Co., Ltd. (Suwon, Korea). The fruits of *P. multiflorus* var. *albus* cultivated in Egypt were purchased from the Weihai Solim trading Co., Ltd. (Beijing, China) in March 2019. The material was authenticated by one of the authors (K.H.K.) and Dongkook Pharm. Co., Ltd. A voucher specimen of the material (DKB117-PM-2018-0814) was deposited at the R&D Center, Dongkook Pharm. Co., Ltd.

3.2. Extraction and Isolation

The fruits (1 kg) of *P. multiflorus* var. *albus* were cut into small pieces and then extracted twice with 5-fold volumes of 30% ethanol (*v/v*) at 80 °C for 10 h. The extracts were filtered, and the filtrate was concentrated using a rotary evaporator. The resultant extract was fully dried by freeze-drying to obtain the crude ethanolic extract powder (110 g). The extract powder (100 g) was suspended in 700 mL of distilled water and then sequentially partitioned with hexane, MC, EtOAc, and *n*-butanol three times. Four major fractions with different polarities were obtained: hexane-soluble (31 mg), MC-soluble (195 mg), EtOAc-soluble (49 mg), and BuOH-soluble (2.4 g) fractions. The isolation procedure for the compounds was conducted by monitoring via TLC and LC/MS-based analysis. First, the hexane-soluble fraction (31 mg) was applied to Sephadex LH-20 column chromatography and eluted with 100% methanol, yielding two fractions (H_A and H_B). Subfraction H_A (14 mg) was purified by semi-preparative HPLC (MeOH/H₂O, 65:35) to isolate compounds 2 (t_R 22.4 min, 0.7 mg) and 3 (t_R 34.8 min, 0.5 mg). However, the isolation of compounds

without any impurities failed in the MC-soluble fraction. The EtOAc-soluble fraction (49 mg) was separated directly by semi-preparative reversed HPLC with a gradient solvent system from 30% MeOH/H₂O to 43% MeOH/H₂O for 80 min to purify compound **1** (*t_R* 37.5 min, 2.3 mg). Finally, the BuOH-soluble fraction (2.4 g) was subjected to reverse-phase MPLC using a gradient solvent system from 5% MeOH/H₂O to 100% MeOH/H₂O for 90 min to obtain three fractions (B_A, B_B, and B_C). Subfraction B_A (1.1 g) was subjected to reverse-phase MPLC using a different gradient solvent system from 5% MeOH/H₂O to 30% MeOH/H₂O for 110 min to produce four subfractions (B_{A1}–B_{A4}). Subfraction B_{A2} (45 mg) was separated by semi-preparative HPLC with a gradient solvent system from 20% MeOH/H₂O to 60% MeOH/H₂O for 70 min to give compound **4** (*t_R* 25.5 min, 1.2 mg).

3.3. Cell Culture and Differentiation

C3H10T1/2 mouse MSCs were cultured in Dulbecco's modified Eagle's medium (DMEM) supplemented with 1% penicillin-streptomycin (P/S) and 10% fetal bovine serum (FBS) at 37 °C in a 5% CO₂ incubator. For adipogenic differentiation, C3H10T1/2 cells were plated in a 6-well plate (a density of 5 × 10⁵ cells/mL). The cells were then treated with 1 μM dexamethasone, 5 μg/mL insulin, 10 μM troglitazone, and 0.5 mM 3-isobutyl-1-methylxanthine for 48 h. Subsequently, the cells were cultured for an additional 72 h with 5 μg/mL insulin and 10 μM troglitazone. During osteogenesis, 20 μM of compounds **1–4** was added to the cells, and resveratrol (20 μM) was used as a positive control. For osteogenic differentiation, C3H10T1/2 cells were exposed to DMEM (5% FBS, 1% P/S) containing 50 μg/mL ascorbic acid and 10 mM β-glycerophosphate for 9 days. During osteogenic differentiation, 20 μM of compounds **1–4** was added to the cells, and 5 μM oryzavitol A was used as a positive control.

3.4. Oil Red O Staining

Cultured cells were washed with phosphate-buffered saline and fixed in 10% neutral-buffered formalin at room temperature for 1 h. The cells were then stained with 0.5% filtered ORO stock solution (Sigma, Saint Louis, MO, USA) in isopropanol. To evaluate the intracellular triglyceride content, the stained cells were redissolved with isopropanol. The absorbance at a wavelength of 520 nm was measured.

3.5. Alkaline Phosphatase Staining

Cultured cells were washed with 2 mM MgCl₂ and then incubated with ALP buffer (100 mM Tris-HCl, pH 9.5; 100 mM NaCl, 0.05% Tween-20, and 10 mM MgCl₂). The cells were then incubated in an ALP buffer containing 0.2 g/mL of 5-bromo-4-chloro-3-indolyl phosphate (Sigma, USA) and 0.4 mg/mL of nitro-blue tetrazolium (Sigma, USA). After washing with 0.5 mM of ethylenediaminetetraacetic acid, the cells were fixed by 10% neutral-buffered formalin.

3.6. mRNA Isolation and Real-Time PCR

RNA was isolated from the cells via NucleoZOL reagent (NucleoZOL; Macherey-Nagel GmbH & Co., KG, Dylan, Germany). Then, complementary DNA (cDNA) was synthesized from total RNA (0.5 μg) by a ReverTraAce qPCR RT Master Mix Kit (FSQ-201; Toyobo, Osaka, Japan) with random primers. The synthesized cDNA was mixed with the amplification mixture including the Thunderbird SYBR qPCR Mix (Toyobo) and primers. The cDNA was then subjected to 40 PCR amplification cycles by a Thermal Cycler Dice (Takara, Kusatsu City, Japan). The results were normalized to the expression of 36b4. The primers used in this study are as follows:

Acidic ribosomal phosphoprotein P0 (36b4): forward 5'-AGATGCAGCAGATCCGCAT-3', reverse 5'-GTTCTTGCCCATCAGCACC-3'; ALP: forward 5'-CCATTCTGGCCACCAAC-3', reverse 5'-AATGCGAGTGGTCTTCCATCA-3'; osteopontin (OPN): forward 5'-CTGGCAGC-TCAGAGGAGAAG-3', reverse 5'-CAGCATTCTGTGGCGCAAG-3'.

3.7. Statistical Analysis

Each sample was tested in triplicate, and the test was repeated three times. Data are expressed as the mean \pm standard deviation (SD). Differences between the control and experimental groups were analyzed via a two-tailed unpaired Student's *t*-test, and statistical significance was defined as $p < 0.05$.

4. Conclusions

In the present study, the phytochemical exploration of *P. multiflorus* var. *albus* fruits resulted in the isolation of four compounds: denatonium (1), *trans*-ferulic acid ethyl ester (2), eugenin (3), and α -L-glutamyl-L-Leucine (4). The chemical structures of isolates 1–4 were elucidated by 1D and 2D NMR, HR-ESIMS, and LC/MS analyses. Intriguingly, to the best of our knowledge, denatonium (1), which is known to be the most bitter chemical compound, was identified from natural sources for the first time, and compounds 2–4 were reported for the first time from *P. multiflorus* var. *albus* in this study; however, compound 2 turned out to be an artifact produced by the extraction with ethanol. Compound 4 exhibited the dual functions of inhibiting adipogenesis and promoting osteogenesis, showing regulatory effects on MSC differentiation. Although the stimulatory effect of the active compounds on osteogenic differentiation was far behind that of the positive control, oryzativol A and compounds 1 and 4 apparently helped promote the differentiation of MSCs into osteocytes.

Supplementary Materials: 1D and 2D NMR spectra of denatonium (1) and general experimental procedures are available online at <https://www.mdpi.com/article/10.3390/plants10102205/s1>, Figure S1: HR-ESIMS data of 1, Figure S2: ^1H NMR spectrum of 1 (CD_3OD , 850 MHz), Figure S3: ^{13}C NMR spectrum of 1 (CD_3OD , 212.5 MHz), Figure S4: ^1H - ^1H COSY spectrum of 1 (CD_3OD), Figure S5: HSQC spectrum of 1 (CD_3OD), Figure S6: HMBC spectrum of 1 (CD_3OD), Figure S7: The total ion chromatogram of ethanol and methanol that we used for extraction in positive ion mode by UPLC-QTOF MS.

Author Contributions: Conceptualization, J.K.K. and K.H.K.; formal analysis, Y.H.L., J.-H.H., K.H.P., S.-H.K., J.-C.K., D.H.K., Y.H.P., and K.W.L.; investigation, Y.H.L., J.-H.H., and K.H.P.; writing—original draft preparation, S.-H.K. and K.H.K.; writing—review and editing, J.K.K. and K.H.K.; visualization, J.-H.H. and S.-H.K.; supervision, J.K.K. and K.H.K.; project administration, J.K.K. and K.H.K.; funding acquisition, K.H.K. All authors have read and agreed to the published version of the manuscript.

Funding: This work was supported by a National Research Foundation of Korea (NRF) grant funded by the Korean government (2019R1A5A2027340 and 2021R1A2C2007937) and the Korea Institute of Science and Technology intramural research grant (2E31311). This work was also supported by the Nano Convergence Industrial Strategic Technology Development Program (20000105, Development of Cosmeceutical Material Platform using Organo-Nano Complexes based on Natural Active Compounds) funded by the Ministry of Trade, Industry & Energy (MOTIE, Korea).

Institutional Review Board Statement: Not applicable.

Informed Consent Statement: Not applicable.

Conflicts of Interest: The authors declare no conflict of interest.

References

1. Meng, J.; Bai, Z.; Huang, W.; Liu, Y.; Wang, P.; Nie, S.; Huang, X. Polysaccharide from white kidney bean can improve hyperglycemia and hyperlipidemia in diabetic rats. *Bioact. Carbohydr. Diet. Fibre* **2020**, *24*, 100222. [[CrossRef](#)]
2. Mojica, L.; de Mejía, E.G. Characterization and comparison of protein and peptide profiles and their biological activities of improved common bean cultivars (*Phaseolus vulgaris* L.) from Mexico and Brazil. *Plant Foods Hum. Nutr.* **2015**, *70*, 105–112. [[CrossRef](#)]
3. Neil, E.S.; McGinley, J.N.; Fitzgerald, V.K.; Lauck, C.A.; Tabke, J.A.; Streeter-McDonald, M.R.; Yao, L.; Broeckling, C.D.; Weir, T.L.; Foster, M.T. White kidney bean (*Phaseolus Vulgaris* L.) consumption reduces fat accumulation in a polygenic mouse model of obesity. *Nutrients* **2019**, *11*, 2780. [[CrossRef](#)]
4. Li, M.; Liu, Q.; Cui, Y.; Li, D.; Wang, H.; Ng, T.B. Isolation and characterization of a *Phaseolus vulgaris* trypsin inhibitor with antiproliferative activity on leukemia and lymphoma cells. *Molecules* **2017**, *22*, 187. [[CrossRef](#)] [[PubMed](#)]

5. E Lacerda, R.R.; do Nascimento, E.S.; de Lacerda, J.T.J.G.; da Silva Pinto, L.; Rizzi, C.; Bezerra, M.M.; Pinto, I.R.; Pereira Filho, S.M.; Pinto, V.d.P.T.; Cristino Filho, G. Lectin from seeds of a Brazilian lima bean variety (*Phaseolus lunatus* L. var. *cascavel*) presents antioxidant, antitumour and gastroprotective activities. *Int. J. Biol. Macromol.* **2017**, *95*, 1072–1081. [PubMed]
6. Jabir, A.S.; Iraby, A.G. Studying the effect of anti-amylase inhibitor extracted from white kidney bean (*Phaseolus vulgaris*) in treat diabetes and obesity in an affected mice. *Int. J. Curr. Microbiol. App. Sci* **2014**, *3*, 97–106.
7. Barrett, M.L.; Udani, J.K. A proprietary alpha-amylase inhibitor from white bean (*Phaseolus vulgaris*): A review of clinical studies on weight loss and glycemic control. *Nutr. J.* **2011**, *10*, 1–10. [CrossRef]
8. Kim, D.H.; Park, Y.H.; Lee, J.S.; Jeong, H.I.; Lee, K.W.; Kang, T.H. Anti-obesity effect of DKB-117 through the inhibition of pancreatic lipase and α -amylase activity. *Nutrients* **2020**, *12*, 3053. [CrossRef]
9. MacMillan, J.; Pryce, R. Further investigations of gibberellins in *Phaseolus multiflorus* by combined gas chromatography-mass spectrometry—the occurrence of gibberellin A20 (pharbitis gibberellin) and the structure of compound b. *Tetrahedron Lett.* **1968**, *9*, 1537–1542. [CrossRef]
10. MacMillan, J.; Seaton, J.; Suter, P. Plant hormones—I: Isolation of gibberellin A1 and gibberellin A5 from *Phaseolus multiflorus*. *Tetrahedron* **1960**, *11*, 60–66. [CrossRef]
11. MacMillan, J.; Pryce, R. Plant hormones—IX: Phaseic acid, a relative of abscisic acid from seed of *Phaseolus multiflorus*. Possible structures. *Tetrahedron* **1969**, *25*, 5893–5901. [CrossRef]
12. MacMillan, J.; Suter, P. The structure of a C12-acid from the seed of *Phaseolus multiflorus*. *Tetrahedron* **1967**, *23*, 2417–2419. [CrossRef]
13. Lee, S.R.; Kang, H.; Yoo, M.J.; Yu, J.S.; Lee, S.; Yi, S.A.; Beemelmans, C.; Lee, J.; Kim, K.H. Anti-adipogenic pregnane steroid from a Hydractinia-associated fungus, *Cladosporium sphaerospermum* SW67. *Nat. Prod. Sci.* **2020**, *26*, 230–235.
14. Yu, J.S.; Park, M.; Pang, C.; Rashaan, L.; Jung, W.H.; Kim, K.H. Antifungal phenols from *Woodfordia uniflora* collected in Oman. *J. Nat. Prod.* **2020**, *83*, 2261–2268. [CrossRef]
15. Lee, S.; Lee, D.; Ryoo, R.; Kim, J.-C.; Park, H.B.; Kang, K.S.; Kim, K.H. Calvatianone, a sterol possessing a 6/5/6/5-fused ring system with a contracted tetrahydrofuran B-ring, from the fruiting bodies of *Calvatia nipponica*. *J. Nat. Prod.* **2020**, *83*, 2737–2742. [CrossRef] [PubMed]
16. Trinh, T.A.; Park, E.-J.; Lee, D.; Song, J.H.; Lee, H.L.; Kim, K.H.; Kim, Y.; Jung, K.; Kang, K.S.; Yoo, J.-E. Estrogenic activity of sanguin H-6 through activation of estrogen receptor α coactivator-binding site. *Nat. Prod. Sci.* **2019**, *25*, 28–33. [CrossRef]
17. Yu, J.S.; Li, C.; Kwon, M.; Oh, T.; Lee, T.H.; Kim, D.H.; Ahn, J.S.; Ko, S.-K.; Kim, C.S.; Cao, S. Herqueilenone A, a unique rearranged benzoquinone-chromanone from the hawaiian volcanic soil-associated fungal strain *Penicillium herquei* FT729. *Bioorg. Chem.* **2020**, *105*, 104397. [CrossRef] [PubMed]
18. Ha, J.W.; Kim, J.; Kim, H.; Jang, W.; Kim, K.H. Mushrooms: An important source of natural bioactive compounds. *Nat. Prod. Sci.* **2020**, *26*, 118–131.
19. Lee, S.; Ryoo, R.; Choi, J.H.; Kim, J.-H.; Kim, S.-H.; Kim, K.H. Trichothecene and tremulane sesquiterpenes from a hallucinogenic mushroom *Gymnopilus junonius* and their cytotoxicity. *Arch. Pharm. Res.* **2020**, *43*, 214–223. [CrossRef] [PubMed]
20. Bolling, B.W.; Parkin, K.L. Phenolic derivatives from soy flour ethanol extract are potent in vitro quinone reductase (QR) inducing agents. *J. Agric. Food Chem.* **2008**, *56*, 10473–10480. [CrossRef] [PubMed]
21. Ali, A.; Makboul, M.; Attia, A.; Ali, D. Chromones and flavans from *Pancreatium maritimum*. *Phytochemistry* **1990**, *29*, 625–627. [CrossRef]
22. Kasai, T.; Sakamura, S. NMR spectra of glutamic acid-containing dipeptides in relation to sequence determination. *Agric. Biol. Chem.* **1973**, *37*, 2155–2157. [CrossRef]
23. Venditti, A. What is and what should never be: Artifacts, improbable phytochemicals, contaminants and natural products. *Nat. Prod. Res.* **2020**, *34*, 1014–1031. [CrossRef] [PubMed]
24. What is Bitrex? Available online: <https://www.bitrex.com/about-bitrex/what-is-bitrex> (accessed on 3 October 2021).
25. Kwiatkowski, A.; Czerwicka, M.; Smulko, J.; Stepnowski, P. Detection of denatonium benzoate (Bitrex) remnants in noncommercial alcoholic beverages by raman spectroscopy. *J. Forensic Sci.* **2014**, *59*, 1358–1363. [CrossRef]
26. Sibert, J.R.; Frude, N. Bittering agents in the prevention of accidental poisoning: children’s reactions to denatonium benzoate (Bitrex). *Arch. Emerg. Med.* **1991**, *8*, 1–7. [CrossRef]
27. Meyer, M.B.; Benkusky, N.A.; Sen, B.; Rubin, J.; Pike, J.W. Epigenetic plasticity drives adipogenic and osteogenic differentiation of marrow-derived mesenchymal stem cells. *J. Biol. Chem.* **2016**, *291*, 17829–17847. [CrossRef]
28. Yi, S.A.; Lee, J.; Park, S.K.; Kim, J.Y.; Park, J.W.; Lee, M.G.; Nam, K.H.; Park, J.H.; Oh, H.; Kim, S. Fermented ginseng extract, BST204, disturbs adipogenesis of mesenchymal stem cells through inhibition of S6 kinase 1 signaling. *J. Ginseng Res.* **2020**, *44*, 58–66. [CrossRef] [PubMed]
29. Ciuffreda, M.C.; Malpasso, G.; Musarò, P.; Turco, V.; Gnechi, M. Protocols for in vitro differentiation of human mesenchymal stem cells into osteogenic, chondrogenic and adipogenic lineages. In *Mesenchymal Stem Cells*; Springer: New York, NY, USA, 2016; pp. 149–158.
30. Kang, M.-H.; Lee, S.-J.; Lee, M.-H. Bone remodeling effects of Korean Red Ginseng extracts for dental implant applications. *J. Ginseng Res.* **2020**, *44*, 823–832. [CrossRef] [PubMed]